Journal of Molecular Structure 1105 (2016) 389–395

Contents lists available at ScienceDirect

Journal of Molecular Structure

journal homepage: http://www.elsevier.com/locate/molstruc

The different conformations and crystal structures of dihydroergocristine

B. Mönch, W. Kraus, R. Köppen, F. Emmerling*

Federal Institute for Materials Research and Testing (BAM), Richard-Willstätter-Str. 11, D-12489 Berlin, Germany

ARTICLE INFO

Article history:
Received 12 May 2015
Received in revised form
11 August 2015
Accepted 13 October 2015
Available online 21 October 2015

Keywords:
Molecularly imprinted polymer
Ergot alkaloids
Solvatomorphs
Hirshfeld surface

ABSTRACT

The identification of different forms of dihydroergocristine (DHEC) was carried out by crystallization from different organic solvents. DHEC was identified as potential template for molecularly imprinted polymers (MIPs) for the epimeric specific analysis of ergot alkaloids (EAs) in food. DHEC was crystallized from different solvents in order to mimic the typical MIP synthesis conditions. Four new solvatomorphs of DHEC were obtained. All solvatomorphs contain a water molecule in the crystal structure, whereas three compounds contain an additional solvent molecule. Based on the conformation of DHEC a comparison with typical EA molecules was possible. The analysis showed that DHEC is a suitable template for MIPs for EAs.

1. Introduction

Fungi of the genus *Claviceps* are specialized parasites of grasses, rushes and sedges, including forage grasses, corn, wheat, barley, oats, rice, and rye [1]. The most prominent member of the genus *Claviceps* is *C. purpurea*. Infection with these species leads to the formation of dark purplish-black mycelia mass called *sclerotium*. The *sclerotium* itself contains inter alia a number of highly toxic secondary fungal metabolites, the so-called ergot alkaloids (EAs), which can cause severe diseases in humans and animals (e. g. gangrene, paresis → ergotism) after consumption of contaminated food and feed.

The main ergot alkaloids produced by *C. purpurea* are ergometrine, ergotamine, ergosine, ergocristine, α-ergocryptine, and ergocornine, along with their corresponding isomeric forms (-inine-forms) [2]. All these EAs are based on a tetracyclic ergoline ring which is methylated on the N-6 nitrogen atom, substituted on C-8 and possesses a double bond in C9–C10 position. They can be divided into simple lysergamides (ergometrine/-inine) and ergotpeptines (ergosine/inine, ergotamine/-inine, ergocornine/-inine, α-ergocryptine/inine and ergocristine/-inine). While the C8-(*R*)-isomers (suffix "-ine") show a high toxicity, the C8-(*S*)-isomers ("-inine") are considered as biologically less or not active [1,3].

In recent years EAs and their epimer-specific determination have gained increasing importance in preventing poisoning of livestock and consumers and economic losses.

For analysing EAs often methods based on the use of high-performance liquid chromatography in combination with fluorescence detection were used. This requires an efficient clean-up to remove matrix components from the raw extracts. Otherwise the quantification is exacerbated by spectral interferences especially when analysing processed cereal samples. In the literature some of the clean-up methods based on the removal of matrix components by binding the EAs on an adsorbent material [4–8], are described. Another approach is the binding of EAs to a resin, and subsequently eluting the EAs after removing matrix components by washing with a suitable solvent. Therefore, Chromabond® C18 ec SPE cartridges [9], EXtrelut® NT3 columns [10–13] or strong cation exchange (SCX) columns [14,15] were applied. A very selective sample clean-up procedure based on the use of molecularly imprinted polymers (MIPs) as solid-phase extraction materials for analysing EAs was described so far only once [16].

MIPs are synthetic polymers featuring receptor or catalytically active sites. Synthesis of MIPs is commonly based on the formation of reticulated polymers in the presence of templates, which could be the analyte itself or a structurally related substance. Because the EAs vary in their substituents at the C8-position it is reasonable to use a structurally related substance as template instead of using one of the priority EAs. Furthermore, using an EA analogue as template molecule for polymer synthesis leads to the avoidance of

* Corresponding author.
E-mail address: franziska.emmerling@bam.de (F. Emmerling).

http://dx.doi.org/10.1016/j.molstruc.2015.10.008
0022-2860/

inaccuracies in measurements caused by residual template bleeding.

A feasibly and reasonably priced template for the synthesis of MIPs for EAs is Dihydroergocristine (DHEC), which can be obtained from commercial available Dihydroergocristine mesylate (DHEC mesylate, Fig. 1). To form suitable receptor or catalytically active sites for EAs during the imprinting process it is essential that DHEC possess the same configuration of the asymmetric centres as the EAs. Since it is not known in detail whether the configurations of the asymmetric centres are influenced during the synthesis steps, it is necessary to identify the absolute configuration of DHEC, based on single crystal X-ray data. Furthermore, only if the conformation of the DHEC reveals a high degree of shape similarity with those of the EAs a selective interaction between the MIP and the EAs can be ensured. Otherwise during imprinting of the polymer an arrangement of potential binding sites would be generated which is not suitable for the EAs. Therefore it is necessary to verify the shape similarity under the influence of different solvents used for the synthesis. A reliable possibility to prove this requirement approximately is based on the single crystal X-ray analysis. For answering these two questions the crystal structures of DHEC crystallized from different solvents were determined. Here we present the crystal structure of four different solvatomorphs of DHEC, the conformational relation among these structures, and prove the suitability of DHEC as a template for EAs for MIPs.

2. Experimental

2.1. Synthesis of dihydroergocristine

20.3 g (28.7 mmol) Dihydroergocristine mesylate (Teva Czech Industries s.r.o., Opava, Komárov, Czech Republic) were suspended in 200 mL of a 25% ammonia solution (p. A., Merck KGaA, Darmstadt, Germany). Then 1000 mL chloroform (p. A., neoLab Migge Laborbedarf-Vertriebs GmbH, Heidelberg, Germany) were added and the suspension was stirred at ambient temperature until the solid was dissolved. After phase separation the aqueous layer was extracted twice with chloroform (1000 mL each). The combined organic layers were washed with 1000 mL brine, subsequently dried over Na_2SO_4 (p. A., Merck KGaA), filtered and evaporated to dryness. The resulting white product was further dried 4 days at 50 °C in vacuo. Codestillation with acetone (CHEMSOLUTE®, Th. Geyer GmbH & Co. KG, Renningen, Germany) and water (Seralpure) was performed to remove small amounts of remaining solvent. Subsequently, the powder was dried again in vacuo for 2 days at 70 °C to give 15.1 g (24.7 mmol, 85.8%) dihydroergocristine.

M.p.: 180.7–181.6 °C. **Elemental composition**: calc. for $C_{35}H_{41}N_5O_5 \times H_2O$ (%): C, 66.75; H, 6.88; N, 11.12; found: C, 66.22; H, 6.85; N, 10.91. **HR-MS**: calc. for $C_{35}H_{42}N_5O_5^+$ 612.3181; found 612.3180 [M + H$^+$]. **^{1}H NMR** (**600 MHz**, **CD_3OD**, **ppm**) δ: 7.37–7.34 (m, 2H, H-18′/22′), 7.22–7.18 (m, 2H, H-19′/21′), 7.15 (dt, J = 8.2, 0.7 Hz, 1H, H-14), 7.14–7.10 (m, 1H, H-20′), 7.09 (dd, J = 8.1, 7.1 Hz, 1H, H-13), 6.91 (d, J = 1.5 Hz, 1H, H-2), 6.86 (ddd, J = 7.3, 1.4, 0.6 Hz, 1H, H-12), 4.68 (t, J = 5.8 Hz, 1H, H-5′), 3.83 (dd, J = 9.2, 6.8 Hz, 1H, H-11′), 3.59–3.52 (m, 1H, H-8′$_A$), 3.52–3.47 (m, 1HH-8′$_B$), 3.44 (dd, J = 14.6, 4.3 Hz, 1H, H-4$_A$), 3.33 (dd, J = 14.1, 6.1 Hz, 1H, H-16′$_A$), 3.21 (dd, J = 14.0, 5.5 Hz, 1H, H-16′$_B$), 3.04 (ddd, J = 11.5, 3.8, 2.0 Hz, 1H, H-7$_A$), 2.97–2.90 (m, 1H, H-10), 2.93–2.87 (m, 1H, H-8), 2.84–2.76 (m, 1H, H-9$_A$), 2.64 (ddd, J = 14.6, 11.1, 1.8 Hz, 1H, H-4$_B$), 2.49 (s, 3H, H-17), 2.46 (t, J = 11.6 Hz, 1H, H-7$_B$), 2.20 (ddd, J = 11.2, 9.9,4.3 Hz, 1H, H-5) 2.16–2.12 (m, 1H, H-13′), 2.13 (dd, J = 13.6, 6.8 Hz, 1H, H-10′$_A$), 2.12–2.08 (m, 1H, H-10′$_B$), 2.07–1.99 (m, 1H, H-9′$_A$), 1.92–1.80 (m, 1H, H-9′$_B$), 1.61 (q, J = 12.5 Hz, 1H, H-9$_B$), 1.12 (d, J = 6.7 Hz, 3H, H-14′/15′), 0.96 (d, J = 6.8 Hz, 3H, H-14′/15′). **^{13}C NMR** (**151 MHz**, **CD_3OD**, **ppm**) δ: 178.2 (C-18), 167.9 (C-3′), 167.2 (C-6′), 139.9 (C-17′), 135.1 (C-15), 132.8 (C-11), 131.0 (C-18′/C-22′), 129.0 (C-19′/C-21′), 127.3 (C-20′), 127.3 (C-16), 123.5 (C-13), 119.4 (C-2), 113.5 (C-12), 111.2 (C-3), 109.9 (C-14), 105.1 (C-12′), 92.2 (C-2′), 68.4 (C-5), 65.3 (C-11′), 59.8 (C-7), 58.2 (C-5′), 47.4 (C-8′), 43.3 (C-8), 43.2 (C-17), 40.9 (C-10), 40.3 (C-16′), 35.1 (C13′), 32.4 (C-9), 27.7 (C-4), 27.3 (C-10′), 23.1 (C-9′), 17.2 (C-14′/15′), 16.1 (C-14′/C-15′). **IR** (**microscope**, **cm^{-1}**): 3620, 3425, 3339, 2945, 2806, 1710, 1668, 1643, 1632, 1533, 1443, 1225, 1209, 1036, 1015.

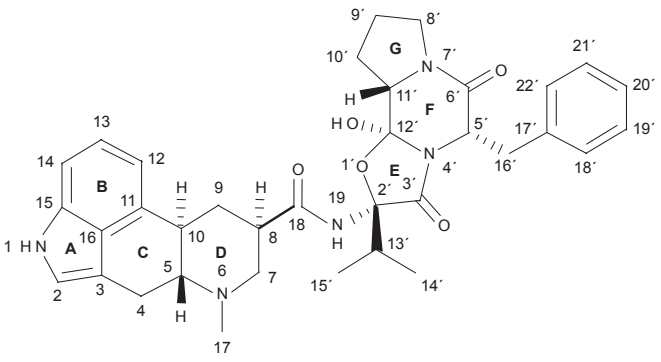

Fig. 1. Chemical structure of DHEC with the numbering system used for characterization.

2.2. Crystallization of dihydroergocristine

Dihydroergocristine was crystallized from various solvents (methanol, chloroform, dichloromethane, acetonitrile), for details see Table 1. Colourless crystals suitable for X-ray analysis were formed after several weeks on slow evaporation of the solvent at ambient temperature in the absence of light.

2.3. Instrumental

The melting point was determined by the capillary tube method using an automatic melting point meter (KSP I N, A. Krüss Optronic, Hamburg, Germany). Elemental analysis was conducted using a vario MACRO elemental analyzer (Elementar Analysensysteme GmbH, Hanau, Germany). The NMR spectra were recorded on a Bruker Avance 600 MHz (Bruker Corporation, Billerica, USA) with the CD_3OD peak as internal standard. Carbons were assigned based on two dimensional NMR analysis (H,H-COSY, HSQC, HMQC). High-resolution mass spectra were obtained with an Exactive Benchtop Orbitrap™ mass spectrometer (Thermo Scientific™, Bremen, Germany, USA). Infrared spectra were recorded on a Bruker Equinox 55 FT-IR spectrometer (Bruker Corporation, Billerica, USA) in the range of 4.000–800 cm^{-1}. The single crystal X-ray data were collected at room temperature using a Bruker AXS SMART diffractometer with an APEX CCD area detector (Mo Kα radiation, graphite monochronator, λ = 0.71073 Å). Data reduction and adsorption correction were carried out using the Bruker AXS SAINT and SADABS packages. The structures were solved by direct methods and refined against F^2 by full-matrix least squares calculation using SHELX97 [17].

Table 1
Overview of solvents and masses of Dihydroergocristine used for crystallisation.

Solvent	m_{DHEC} [mg]	$V_{Solvent}$ [μL]
Methanol	4.1	200
Chloroform	5.6	500
Dichloromethane	2.6	1000
Acetonitrile	4.0	200

Anisotropic thermal parameters were employed for non-hydrogen atoms. The hydrogen atoms were treated isotropically with U_{iso} = 1.2 times the U_{eq} value of the parent atom. The Hydrogen atoms were placed in calculated positions, allowing them to ride on their parent C atoms with Uiso(H) = 1.2 Ueq(C). Crystal data and structure refinement details are summarized in Table 1. The crystallographic data of the structures have been deposited with the Cambridge Crystallographic Data Centre as supplementary publications. CCDC 1020057–1020060 contains the supplementary crystallographic data for this paper. These data can be obtained free of charge via http://www.ccdc.cam.ac.uk/conts/retrieving.html (or from the Cambridge Crystallographic Data Centre, 12, Union Road, Cambridge CB2 1EZ, UK; fax: +44 1223 336033). The CCDC numbers [23] are listed in Table 2.

Powder diffraction measurements were performed on a D8 Discover diffractometer (Bruker AXS, Karlsruhe, Germany) equipped with a Lynxeye detector and operated in transmission geometry (Cu $K_{\alpha 1}$ radiation. λ = 0.154056 nm). The samples were sealed in a glass capillary of 0.5 mm diameter (WJM-Glas, Müller GmbH, Berlin, Germany) and the powder diffraction measurements were conducted over a 2θ range of 5–50° with a step size of 0.009° and 0.5 s per step at room temperature. The obtained powder patterns display a very good correlation with the calculated pattern from the determined structures (see Fig. S1).

3. Results

Colourless crystals of compound **1**–**4** were obtained after slow evaporation of the solvent methanol (compound **1**), chloroform (compound **2**), dichloromethane (compound **3**), and acetonitrile (compound **4**) at ambient temperature. Compound **1** contains an additional water molecule in the asymmetric unit. The other three analysed compounds **2**–**4** contain a water molecule and an additional solvent molecule in the crystal structure.

The molecular configuration of DHEC crystallized from different solvents is comparable in all crystal structures. The compounds **1**–**4** crystallize in the same configuration with chiral centres at C5, C10, C8, C2′, C12′, C11′ and C5′. For compound **2** and **3** the absolute configuration could be determined since these structures contain a solvent molecule with a heavy atom [18]. The final value of the Flack parameter was 0.00(4) for compound **2** respectively 0.00(11) for compound **3**. The absolute chirality at the chiral centres was determined as: C5(R), C10(R), C8(R), C2′(R), C12′(S), C11′(S), C5′(S). The obtained chirality is in agreement with that found in related structures [19,20].

As an example for the obtained structures of compound **1**–**4** the molecular configuration of compound **3** is shown in Fig. 2 (for structures of compound **1**, **2** and **4** see supplementary information).

The ergoline rings, forming the indole moiety (ring A and B), are nearly planar, such as ring E and G (see Fig. 2). The plane displacement (rms) vary from 0.0047 to 0.0098 Å. The non-aromatic ring C of the ergoline skeleton (C3–C4–C5–C10–C11–C16) and the piperazine part of the tripeptide moiety (ring F, C5′–C6′–N7′–C11′–C12′–N4′) adopt an envelope E_6 conformation. Ring D (C5–N6–C7–C8–C9–C10) has a regular chair conformation. A hydrogen bond between the hydroxyl group (O4) and the amide carbonyl oxygen (O1) could be determined as an intramolecular interaction for all the four structures with distances in the range of 2.759–2.796 Å for d_{O4-O1} and 1.997–2.054 Å for d_{O4H-O1} and the corresponding angle from 150.36 to 154.50° (for details see Table 3).

The solvatomorphs **1**–**4** crystallize in the non-centrosymmetric orthorhombic space group $P2_12_12_1$ with four formula units in the unit cell and a cell volume ranging from 3312.6 to 3775.2 Å^3 (see Table 2). In contrast, the already known dioxan solvatomorph of DHEC QABBUQ [19]; crystallizes in the monoclinic space group $P2_1$ with two molecules in the unit cell and a cell volume of 2091.1 Å^3.

When comparing the crystal structure known from literature with the crystal structure of compound **1**–**4** three types of packing arrangement can be distinguished. The conformation of the DHEC molecule differs regarding to the position of the phenyl ring, the part with the highest degree of freedom within the molecule. In Fig. 3 the three different conformations are depicted in an overlay representation. The solvents incorporated in the crystal structure influence the packing motif. Three types of crystal packing regarding the interactions between the molecules and the dimensionality the formed network can be identified (Type I–III). Common for all structures is the absence of π–π interactions. This might be a reason for an unconstrained packing and different conformations (see Supporting information, Figs. S1–S4).

Type I: The crystal structure of QABBUQ [19] contains two molecules of 1,4-Dioxane per DHEC molecule. One molecule of 1,4-Dioxane interacts with a DHEC molecule via hydrogen bonds between the N1 atom of the indole moiety to the oxygen of the dioxane with a distance of d_{N1-O} 2.988 Å (for detailed information

Table 2
Selected crystallographic data and structure refinement parameters of compounds **1**–**4**.

Compound reference	**1**	**2**	**3**	**4**
Chemical formula	$C_{35}H_{41}N_5O_5 \cdot H_2O$	$C_{35}H_{41}N_5O_5 \cdot CHCl_3 \cdot H_2O$	$C_{35}H_{41}N_5O_5 \cdot CH_2Cl_2 \cdot H_2O$	$C_{35}H_{41}N_5O_5 \cdot C_2H_3N \cdot H_2O$
Formula mass	629.74	749.11	714.67	669.79
Crystal system	Orthorhombic	Orthorhombic	Orthorhombic	Orthorhombic
a/Å	8.9068(9)	10.0319(11)	9.6940(17)	9.6837(7)
b/Å	17.3351(17)	14.3662(16)	14.084(3)	14.0741(10)
c/Å	21.455(2)	26.195(3)	26.075(5)	26.3065(17)
Unit cell volume/Å^3	3312.6(6)	3775.2(7)	3560.1(12)	3585.3(4)
Temperature/K	296(2)	296(2)	296(2)	296(2)
Space group	$P2_12_12_1$	$P2_12_12_1$	$P2_12_12_1$	$P2_12_12_1$
No. of formula units per unit cell, *Z*	4	4	4	4
Radiation type	Mo Kα	Mo Kα	Mo Kα	Mo Kα
Absorption coefficient, μ/mm^{-1}	0.087	0.293	0.235	0.085
No. of reflections measured	29,052	32,599	30,084	32,482
No. of independent reflections	8319	9186	8912	8739
R_{int}	0.0658	0.0674	0.0902	0.1172
Final R_1 values ($I > 2\sigma(I)$)	0.0572	0.0835	0.0625	0.0739
Final $wR(F^2)$ values ($I > 2\sigma(I)$)	0.1404	0.2202	0.1506	0.1746
Final R_1 values (all data)	0.0740	0.1495	0.1128	0.1162
Final $wR(F^2)$ values (all data)	0.1540	0.2494	0.1703	0.2006
Goodness of fit on F^2	1.052	0.901	0.898	1.005
Flack parameter	−0.5(6)	0.00(4)	0.00(11)	−0.4(9)
CCDC number	1020060	1020057	1020058	1020059

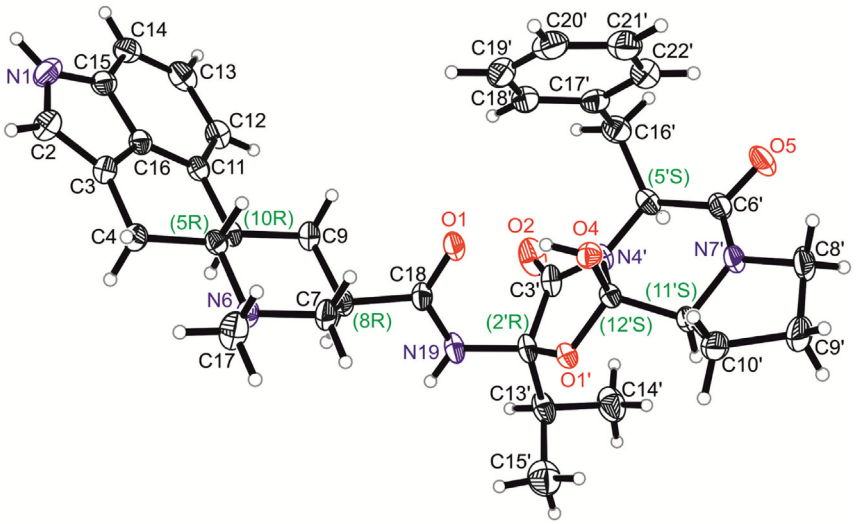

Fig. 2. Ortep representation and numbering scheme of the DHEC molecule in compound **3** [21]. The displacement ellipsoids are shown with 30% probability. The labelling of asymmetric carbon atoms depicted in green. (For interpretation of the references to colour in this figure legend, the reader is referred to the web version of this article.)

Table 3
Distances and angles of the intramolecular hydrogen bonds.

Compound	d_{O4-O1} [Å]	d_{O4H-O1} [Å]	A [°]
1	2.796	2.054	150.36
2	2.780	2.028	152.32
3	2.769	2.014	152.92
4	2.759	1.997	154.50

see Table S1, supporting information). No interactions between the DHEC molecules and the second 1,4-Dioxane or between two DHEC molecules could be detected (Table 4).

Type II: As mentioned above compound **1** crystallizes with a water molecule in the lattice. The study of the interactions in the crystal lattice indicates the formation of a three dimensional network. The water molecule is involved in the hydrogen bonded network with two intermolecular hydrogen bonds. Three different intermolecular hydrogen bonds connect the DHEC molecules directly and by a water molecule. The first hydrogen bond is formed between the nitrogen atom (N1) of the indole moiety to the oxygen atom (O2) attached to the oxazolidine part with $d_{N1-O2} = 2.864$ Å and $d_{N1H-O2} = 2.037$ Å. A further hydrogen bond is formed between the oxygen atom (O5) bound to the piperazine moiety to the water molecule (O6) (see Fig. 4A) with $d_{O5-O6} = 2.808$ Å and $d_{O6H-O5} = 1.953$ Å. The third hydrogen bond is formed between the nitrogen atom (N19) to the water molecule (O6) with $d_{N3-O6} = 2.999$ Å and $d_{N3H-O6} = 2.147$ Å (for detailed information see Table 5). The resulting structure is shown in Fig. 4A. The compounds **2**–**4** belong to type III. Within this type the DHEC molecules are connected via hydrogen bonds including the bridging crystal water (see Fig. 4A–C). No direct interaction between the DHEC molecules is formed. Three different types of hydrogen bonds can be identified. One hydrogen bond is formed between the oxygen atom of the water molecule and oxygen atom bound to the piperazine moiety with d_{O6-O5} within a range of 2.794–2.840 Å and d_{O6H-O5} 1.905–2.137 Å. Another hydrogen bond is formed between water and the piperidine moiety in the range of d_{O6-N6} 2.827–2.859 Å and d_{O6H-N6} 1.924–1.995 Å. The third hydrogen bond is formed between water and the indole moiety. The corresponding distances are in a range of d_{O6-N1} 2.777–2.855 Å and d_{O6-HN1} 1.928–2.014 Å (for detailed information see Table 5). The corresponding structure motifs involving the connection to the water molecules are shown in Fig. 4

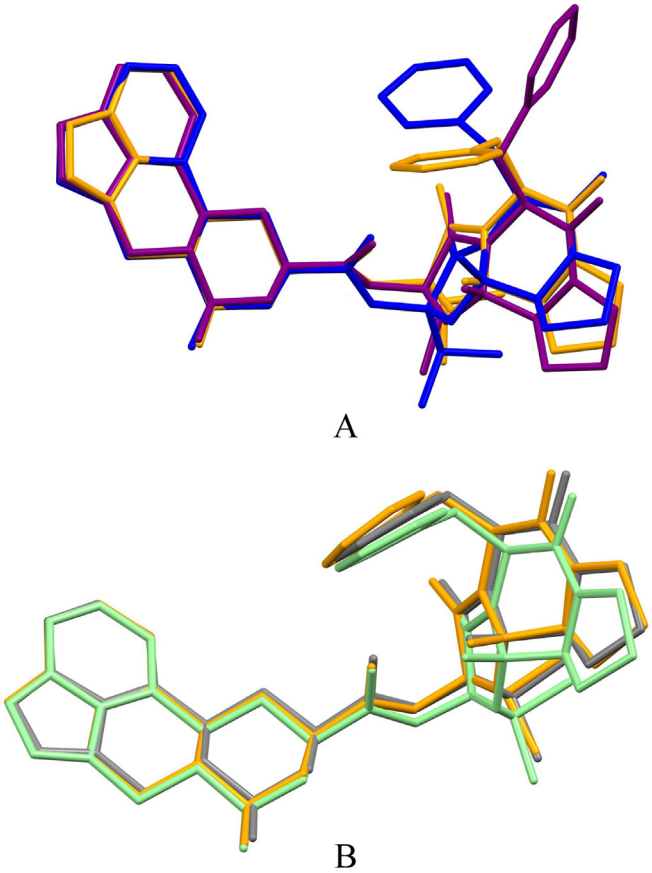

Fig. 3. Stereographic representation showing the overlay of the three DHEC solvatomorphs containing additional solvent molecules in the crystal structure: (A) methanol (purple), chloroform (orange), and 1,4 dioxane (blue; QABBUQ); (B) chloroform (orange), dichloromethane (grey), and acetonitrile (green). (For interpretation of the references to colour in this figure legend, the reader is referred to the web version of this article.)

The resulting structures consist of layers stacked parallel to the a–c-plane. Between these layers cavities for the solvent molecules can be found. The solvent molecules are not involved in the

Table 4
Different dimensionality of the packing of the crystal structures.

Structure type	I	II	III
Compound	QABBUQ [19]	**1**	**2**–**4**
Included Solvent	2× Dioxane molecules	H_2O	H_2O + other
Intramolecular hydrogen bond	+	+	+
Interactions between	1 Dioxane – DHEC	DHEC–DHEC 2× H_2O-DHEC	3× H_2O-DHEC
Network/Packing	Dimers	3D network	2 D Layer structure

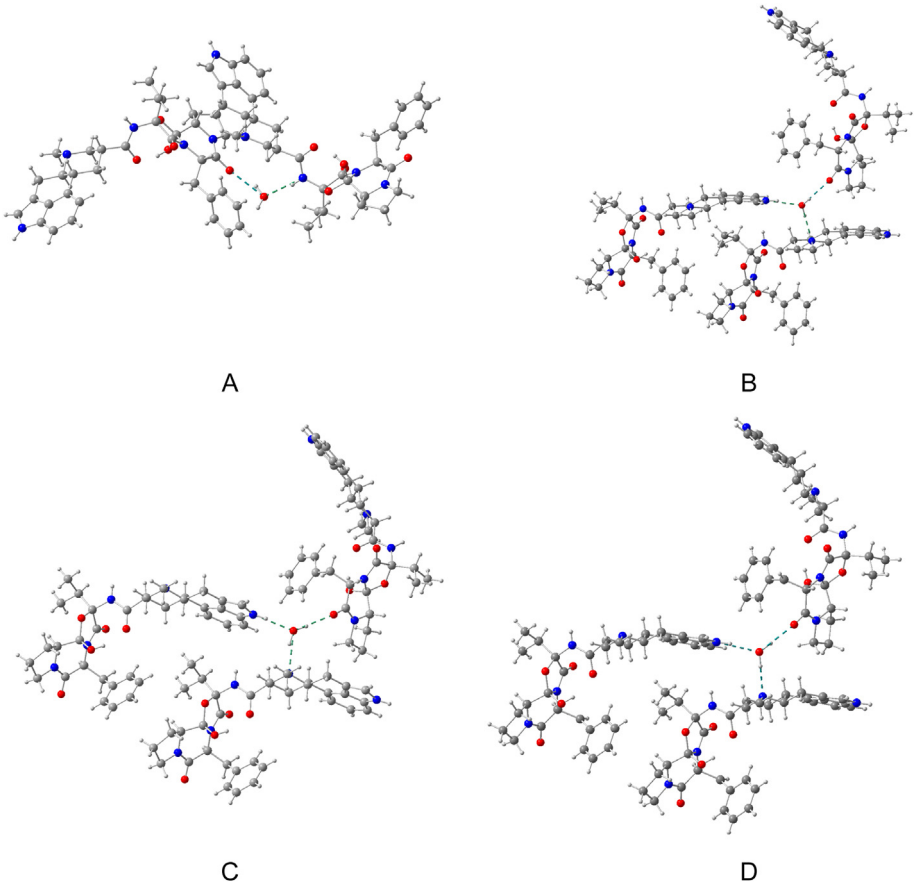

Fig. 4. Obtained structures showing the influence of the water molecules on the packing arrangement (A compound **1**, B compound **2**, C compound **3**, D compound **4**).

Table 5
Intermolecular hydrogen bonds of compound 2, 3 and 4.

Compound	O_{Water}–O5 (piperazine)		O_{Water}–N6 (piperidine)		O_{Water}–N1 (indole)	
	d_{O6-O5} [Å]	d_{O6H-O5} [Å]	d_{O6-N6} [Å]	d_{O6H-N6} [Å]	d_{O6-N1} [Å]	d_{O6-HN1} [Å]
1	2.808	1.953	2.999	2.147	2.864	2.037
2	2.840	2.137	2.859	1.995	2.855	2.014
3	2.825	1.936	2.835	1.961	2.806	1.954
4	2.794	1.905	2.827	1.924	2.777	1.928

interaction between the different layers. In Fig. 5 the possible volume (voids) without the corresponding solvent (water, chloroform) of compound 2 are depicted exemplarily [25]. The potential solvent area in this case would be 671.7 $Å^3$ per unit cell volume of 3775.2 $Å^3$ (17.8%).

Despite these similarities the conformation of the DHEC molecule is slightly different due to the solvent involved in the crystal lattice (see Fig. 4). Depending on the existing solvent in the layer cavities different lattice constants are realized (see Table 1).

Fig. 6 presents the different crystal packing mentioned above and the corresponding powder patterns for compound **2**–**4**. The small changes of the lattice constants lead to a significant shifting of the peaks in the powder pattern.

To estimate the suitability of DHEC as template for EA in the MIP synthesis, a Hirshfeld surface analysis was performed [22–24]. One has to keep in mind that a template should mimic the size respectively the volume and the potential binding sites capable of the EAs. The Hirshfeld surface analysis depicted in Fig. 7 covers the relevant

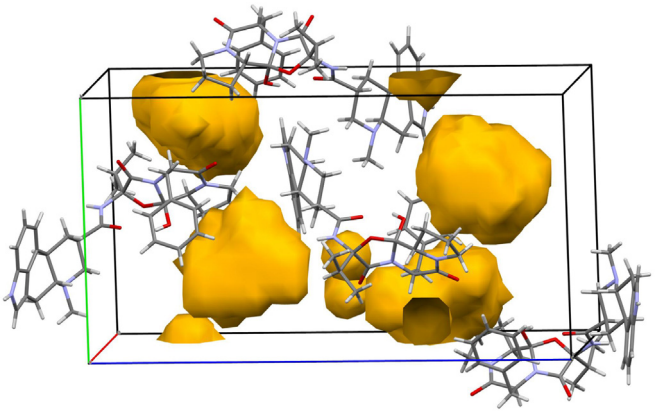

Fig. 5. Voids of compound **2** by excluded solvents.

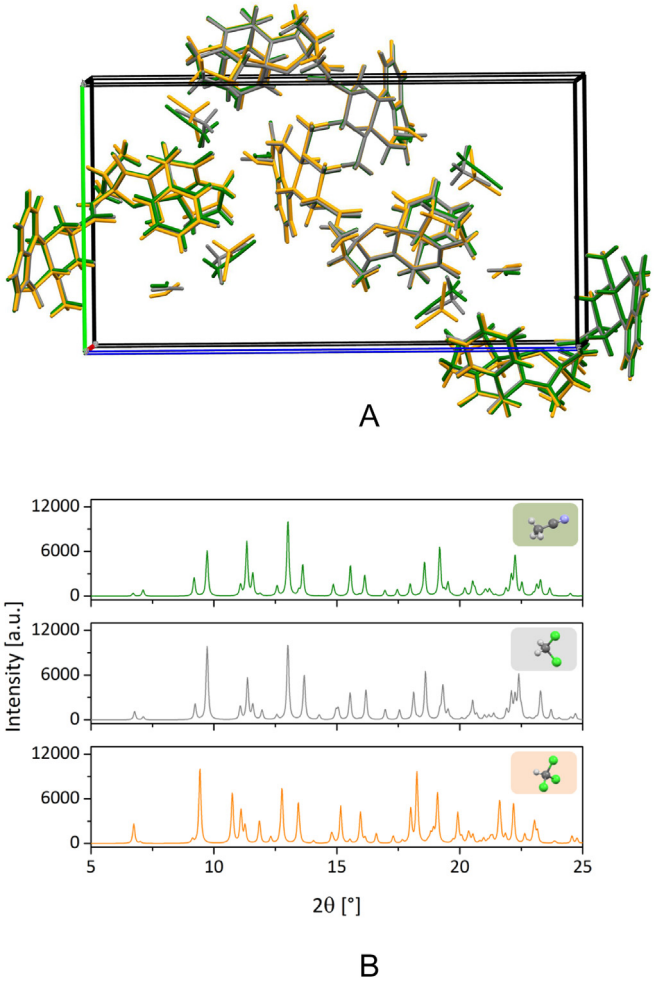

Fig. 6. A) View of the unit cells of compound **2** (orange), **3** (grey) and **4** (green) and B) the corresponding powder patterns (calculated). (For interpretation of the references to colour in this figure legend, the reader is referred to the web version of this article.)

parameters for compound **2** in comparison with ergotamine, a typical EA. It could be seen that the parameters for DHEC are in a very good agreement with the ones for ergotamine. Therefore, DHEC is able to form suitable cavities for EAs during the MIP synthesis process.

The comparison of the calculated electrostatic potentials (Fig. 8) for both substances suggests a good accordance of the binding sites

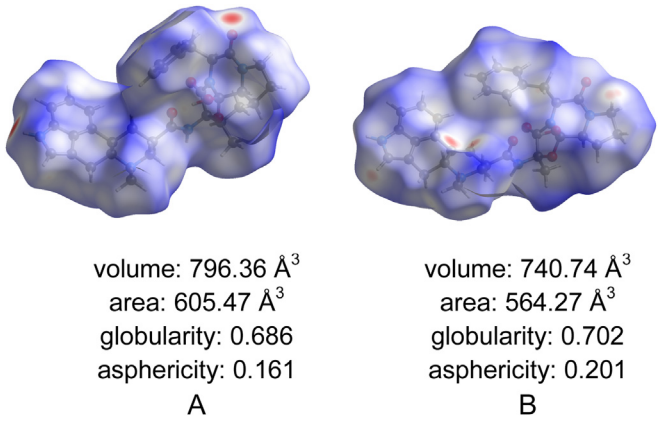

Fig. 7. Hirshfeld surface of compound **2** (A) and ergotamine (B) [25] mapped with d_{norm} over the range of −0.572 and 1.854 The normalized contact distance d_{norm} is defined in terms of d_e, d_i and the vdW radii of the atoms, where d_e is the distance from a point on the surface to the nearest nucleus outside the surface and d_i is the distance from a point on the surface to the nearest nucleus inside the surface. Red colour indicates distances shorter than the sum of vdW radii through white to blue which distances longer than sum of vdW radii (For details see Ref. [24]). (For interpretation of the references to colour in this figure legend, the reader is referred to the web version of this article.)

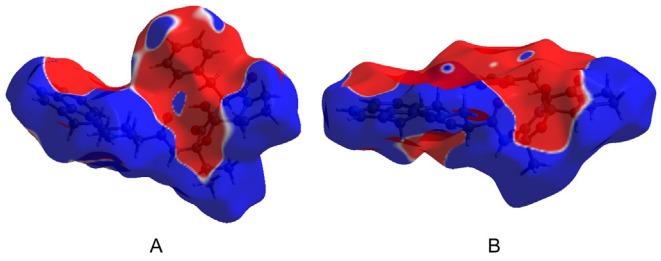

Fig. 8. Electrostatic potential mapped on Hirshfeld surface for compound **2** (A) and ergotamine (B). The potential are mapped over the range of ±0.002 a.u. and were calculated using Gaussian09 and the HF/Midi! − wavefunction [26].

formed during polymerization. The functionalized monomers used should arrange around the template DHEC in a way that the resulting binding sites could interact selective with the corresponding part of EAs.

4. Conclusion

Dihydroergocristine seems to be a suitable template for molecularly imprinted polymers for the epimeric specific analysis of ergot alkaloids. DHEC was crystallized from different solvents and the obtained crystals were characterized by single crystal X-ray analysis. The structural analysis showed that depending on the solvent different solvatomorphs are formed containing DHEC, water molecules and additional solvent molecules in the assymetric unit. These solvatomorphs can be divided into three types of crystal structures in consequence of the different affinity towards forming hydrogen bonds. The obtained structures indicate that the absolute configuration remains unchanged and is in accordance with the expected values. The analysis of the overall geometry, the surface and volume of the DHEC molecule in the different crystal structures confirm that DHEC is a suitable template for mimicking ergot alkaloids for molecularly imprinted polymers.

Appendix A. Supplementary data

Supplementary data related to this article can be found at http://dx.doi.org/10.1016/j.molstruc.2015.10.008.

References

[1] European Food Safety Authority (EFSA), Panel on Contaminants in the Food Chain (CONTAM). Scientific opinion on ergot alkaloids in food and feed, EFSA J. 10 (2012) 2798–2955.
[2] E.L. Komarova, O.N. Tolkachev, The chemistry of peptide ergot alkaloids, part 1. Classification and chemistry of ergot peptides, Pharm. Chem. J. 35 (2001) 304–513.
[3] L. Pierri, I.H. Pitman, I.D. Rae, D.A. Winkler, P.R. Andrews, Conformational analysis of the ergot alkaloids ergotamine and ergotaminine, J. Med. Chem. 25 (1982) 937–942.
[4] C. Müller, S. Kemmlein, H. Klaffke, W. Krauthause, A. Preiss-Weigert, R. Wittkowski, Mol. Nutr. Food Res. 53 (2009) 500–507.
[5] C. Müller, H.S. Klaffke, W. Krauthause, R. Wittkowski, Mycotoxin Res. 22 (2006) 197–200.
[6] R. Krska, G. Stubbings, R. Macarthur, C. Crews, Anal. Bioanal. Chem. 391 (2008) 563–576.
[7] C. Crews, W.A.C. Anderson, G. Rees, R. Krska, Food Addit. Contam. Part B Surveill. 2 (2009) 79–85.
[8] M.K. Kokkonen, M.N. Jestoi, Food Anal. Methods 2 (2009) 128–140.
[9] R. Mohamed, E. Gremaud, J. Richoz-Payot, J.C. Tabet, P.A. Guy, J. Chromatogr. A 1114 (2006) 62–72.
[10] C. Klug, W. Baltes, W. Kronert, R. Weber, Z. Leb. Unters. Forsch. 186 (1988) 108–113.
[11] C. Klug, W. Baltes, W. Kronert, R. Weber, Z. Leb. Unters. Forsch. 179 (1984) 245–246.
[12] J. Wolff, C. Neudecker, C. Klug, R. Weber, Z. Ernährungswiss. 27 (1988) 1–22.
[13] U. Lauber, R. Schnaufer, M. Gredziak, Y. Kiesswetter, Mycotoxin Res. 21 (2005) 258–262.
[14] G.M. Ware, G. Price, L. Carter, R.R. Eitenmiller, J. AOAC Int. 83 (2000) 1395–1399.
[15] R. Köppen, T. Rasenko, S. Merkel, B. Mönch, M. Koch, J. Agric. Food Chem. 61 (2013) 10699–10707.
[16] P. Lenain, J.D. Mavungu, P. Dubruel, J. Robbens, S. De Saeger, Anal. Chem. 84 (2012) 10411–10418.
[17] G.M. Sheldrick, Acta Crystallogr. Sect. A 64 (2008) 112–122.
[18] H.D. Flack, Acta Crystallogr. Sect. A 39 (1983) 876–881.
[19] J. Čejka, B. Kratochvil, A. Jegorov, L. Cvak, Z. Krist. New Cryst. Struct. 212 (1997) 111–112.
[20] J. Čejka, J. Ondráček, M. Hušák, B. Kratochvíl, A. Jegorov, J. Stuchlík, Collect. Czechoslov. Chem. Commun. 60 (1995) 1333–1342.
[21] L.J. Farrugia, J. Appl. Crystallogr. 30 (1997) 565.
[22] F.L. Hirshfeld, Theor. Chim. Acta 44 (1977) 129–138.
[23] M.A. Spackman, P.G. Byrom, Chem. Phys. Lett. 267 (1997) 215–220.
[24] M.A. Spackman, D. Jayatilaka, Cryst. Eng. Comm. 11 (2009) 19–32.
[25] S. Pakhomova, J. Ondracek, M. Husak, B. Kratochvil, A. Jegorov, J. Stuchlík, Acta Crystallogr. Sect. C 51 (1995) 308.
[26] M.J. Frisch, G.W. Trucks, H.B. Schlegel, G.E. Scuseria, M.A. Robb, J.R. Cheeseman, G. Scalmani, V. Barone, B. Mennucci, G.A. Petersson, H. Nakatsuji, M. Caricato, X. Li, H.P. Hratchian, A.F. Izmaylov, J. Bloino, G. Zheng, J.L. Sonnenberg, M. Hada, M. Ehara, K. Toyota, R. Fukuda, J. Hasegawa, M. Ishida, T. Nakajima, Y. Honda, O. Kitao, H. Nakai, T. Vreven, J.A. Montgomery, Jr., J.E. Peralta, F. Ogliaro, M. Bearpark, J.J. Heyd, E. Brothers, K.N. Kudin, V.N. Staroverov, R. Kobayashi, J. Normand, K. Raghavachari, A. Rendell, J.C. Burant, S.S. Iyengar, J. Tomasi, M. Cossi, N. Rega, J.M. Millam, M. Klene, J.E. Knox, J.B. Cross, V. Bakken, C. Adamo, J. Jaramillo, R. Gomperts, R.E. Stratmann, O. Yazyev, A.J. Austin, R. Cammi, C. Pomelli, J.W. Ochterski, R.L. Martin, K. Morokuma, V.G. Zakrzewski, G.A. Voth, P. Salvador, J.J. Dannenberg, S. Dapprich, A.D. Daniels, Ö. Farkas, J.B. Foresman, J.V. Ortiz, J. Cioslowski, D.J. Fox, Gaussian, Inc., Wallingford CT, (2009).